PROCEEDINGS OF SCIENCE

Variations of secondary particle arrival time detected by LHAASO-KM2A during thunderstorms

Xuejian Chen,* Xunxiu Zhou, Ci Yang and Daihui Huang (on behalf of the LHAASO Collaboration)

School of Physical Science and Technology, Southwest Jiaotong University, Chengdu 610031, China

E-mail: zhouxx@swjtu.edu.cn

Abstract: A sub-array of the Large High Altitude Air Shower Observatory (LHAASO), KM2A contains 5216 electromagnetic particle detectors (EDs) and 1188 muon detectors (MDs). For each shower event that meets the trigger conditions (at least 20 fired EDs within a time window of 400 ns) in KM2A array, there are many signals from ED and MD detectors. The information on the arrival time and location of each signal are recorded, and the ED hits are used for shower reconstruction. Due to the acceleration and deflection by the atmospheric electric field (AEF) during a thunderstorm, the arrival time and position of the ground-level particles are modified, resulting in the changes in the inferred shower detection. To understand the shower event variation during thunderstorms, the particle arrival time is studied by analyzing the KM2A data. We can measure the distribution of changes of arrival time in the thunderstorm electric field. The variation amplitude is not only dependent on the AEF, but also highly correlated with the direction of the shower event. With the increase of the AEF strength and the zenith angle, the variation in amplitude of the arrival time becomes larger. Our results are useful in understanding the variation of shower rate detected by LHAASO-KM2A, and will also provide important information for shower reconstruction during thunderstorms.

Keywords: Thunderstorm, Arrival time, LHAASO-KM2A

38th International Cosmic Ray Conference (ICRC2023)
26 July - 3 August, 2023
Nagoya, Japan

*Speaker

1. Introduction

Various particle accelerators operate in the cosmic plasma, filling the galaxy with high-energy particles (primary cosmic rays). Upon entry into the atmosphere, these particles undergo significant interaction with atomic nuclei, producing a large number of secondaries by hadron and electromagnetic cascades. Thunderstorms are common convective weather events accompanied by intense lightning discharges, strong winds and heavy rain [1]. Zhang et al. [2] have developed a charge model that predicts the electric field generated by thundercloud charges through theoretical calculations and simulations. Compared to the electric field strength (<10 V/cm) in fair weather [3], the electric field strength during thunderstorms can be up to 1000 V/cm or even higher [4, 5], and the secondary charged particles of extensive air showers (EAS) are accelerated and deflected by the field, causing the variations in secondary particles measured at ground-level.

Alexeenko et al. [6] found that the flux variation of cosmic rays is related to the intensity of the AEF during thunderstorms, which has also been studied in several ground-based experiments during long-term observations [7-9]. In addition, a few articles have studied the effect of the electric fields on the energy of secondary particles, and found that the energy spectrum is softened in the presence of the field [10-12]. Axikegu et al. [13] simulated the variation in the lateral density of secondary positrons and electrons, and found that the lateral distribution becomes wider. Due to the acceleration and deflection in the electric field, the arrival time distribution of secondary particles will also change during thunderstorms. However, there are few studies on this topic.

In this study, data of the shower mode detected by LHAASO-KM2A are analyzed. In the shower mode, the trigger logic requires at least 20 EDs to be fired within a time window of 400 ns. Notably, any changes of secondary particle arrival time will invariably affect the particle number within the aforementioned time window. As a result, the selection of shower events that meet the trigger condition could be modified. The purpose of this paper is to study the effects of thunderstorm electric fields on the arrival times of secondary particles detected by LHAASO-KM2A.

2. The LHAASO-KM2A experiment

Located on Mt. Haizi in Daocheng, Sichuan Province, P.R. China, LHAASO consists of four sub-arrays, KM2A, WCDA, WFCTA and ENDA [14]. LHAASO will operate for more than 10 years under severe environmental conditions. The signal attenuation is required to be less than 20% in 10 years due to detector aging. As the main part of LHAASO, KM2A contains 5216 EDs and 1188 MDs (as shown in Fig. 1). To study the cosmic ray variations during thunderstorms, two AEF monitors (Boltek EFM-100) were installed at the LHAASO site. One was located on the roof of the WCDA-2 building (here, we call it EFM-1), and the dynamic range of the AEF measurement was from –270 to 270 V/cm [15]. Another one was mounted flush with the surface of the ground (here, we call it EFM-2), with a saturation value of ±1000 V/cm. The positions of EFM-1 and EFM-2 at the LHAASO site are also shown in Fig. 1.

3. Data selection and observation results

The evolution of the lateral spread and energies of secondary particles in an EAS is influenced by the acceleration and deflection in the electric field, as evidenced by various studies [12,13,16].

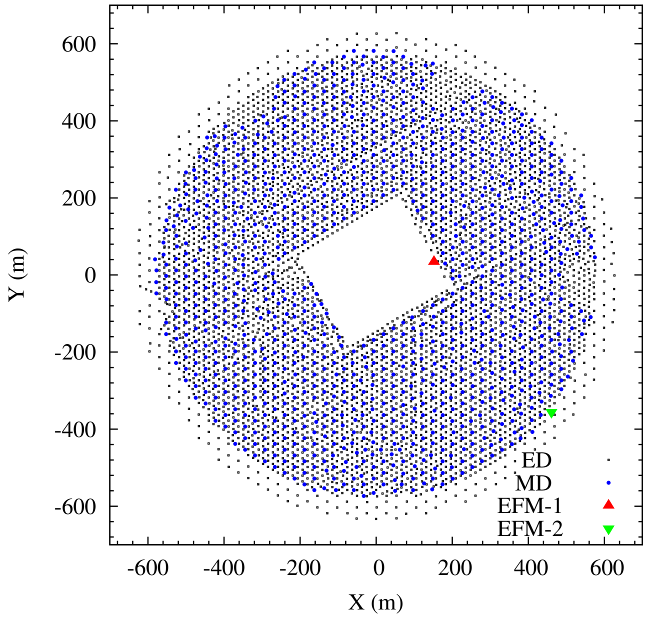

Fig. 1. Layout of LHAASO-KM2A.

That means the time information of the secondary particles will also change. The space-time information can be used to reconstruct the direction of the shower [17]. By using the arrival time distribution of secondary particles in an EAS, Rasterizer et al [18] presented a method to discriminate the mass and energy of primary cosmic rays. So it's useful to study the distribution of secondary particle arrival times.

3.1 The arrival time of secondary particles detected by LHAASO-KM2A

In the LHAASO-KM2A experiment, for each shower event that satisfies the trigger condition, the trigger time is set at 0, and the data acquisition system (DAQ) records all hits within 5000 ns before or after the trigger time. These hits contain secondary particles in the EAS, as well as detector noise. Fig. 2(a) shows the distribution of secondary particle arrival time for one shower event in fair weather. We can see that the secondary particles are mainly concentrated within hundreds of nanoseconds after the trigger time, while the noise is randomly distributed over the entire 10 us.

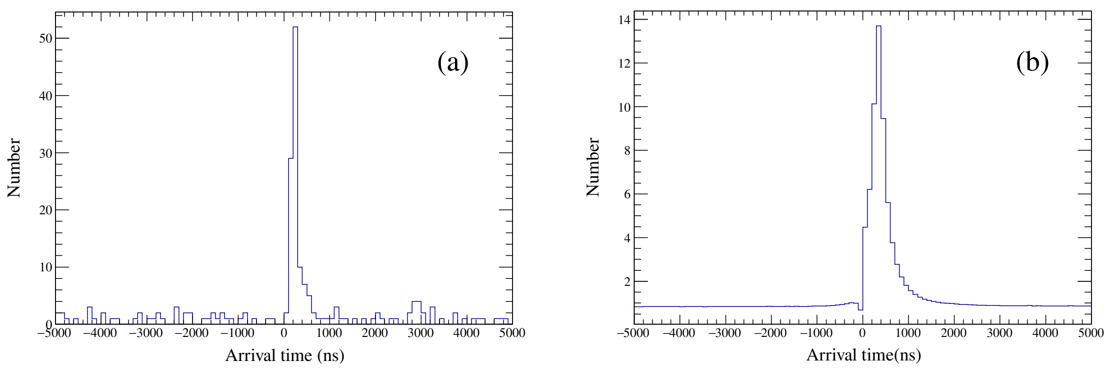

Fig. 2. Arrival time of ground-level particles from one shower event (a) and the average arrival time distribution per shower event (b) in fair weather.

In order to clearly measure the arrival time distribution of secondary particles, many shower data in fair weather are analyzed. Fig. 2(b) shows the average distribution per shower event. We can see that the arrival time of ground-level particles are not random, but show a clear pattern. From -5000 to -1000 ns, the particle number remains essentially stable. From the trigger time, the number increases sharply, reaching a maximum value before 400 ns, and then decreasing rapidly. After 3000 ns, the particle number remains stable again.

3.2 The arrival time variation during thunderstorms

For the thunderstorm that occurred on February 2, 2022 (here, we call it Thunderstorm 20220202), the specific information of AEF variation is presented in Fig. 3. Thunderstorm 20220202 lasted for more than 30 minutes (from 12:00 to 12:36 UT), with a maximum electric field strength more than 400 V/cm. We define the period 11:00-11:50 UT before Thunderstorm 20220202 as fair weather.

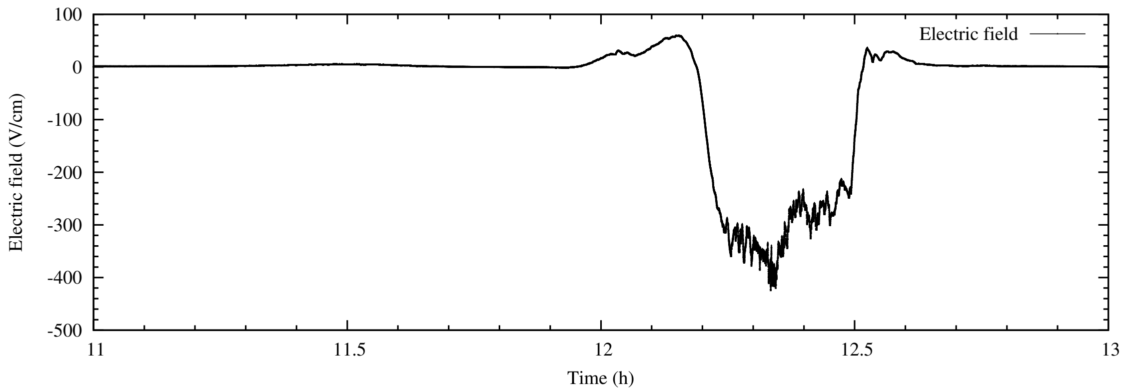

Fig. 3. Variation in the near-earth AEF during Thunderstorm 20220202.

Fig. 4 shows the arrival time distribution of a typical shower event during Thunderstorm 20220202. We find that the time distribution appears to be wider.

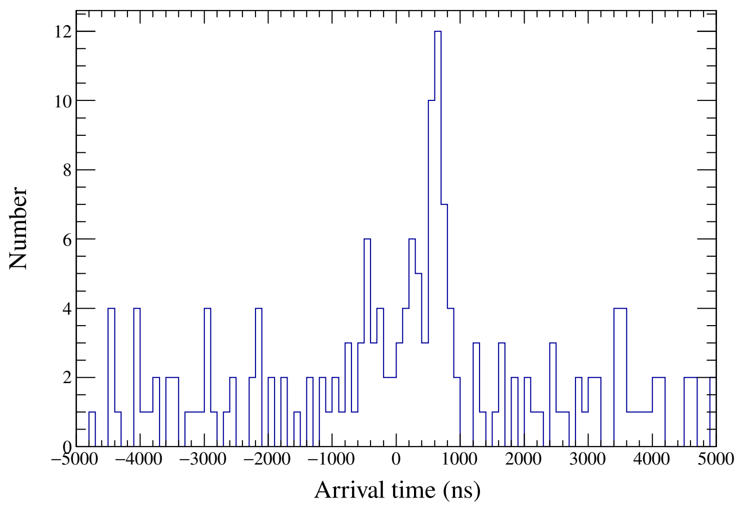

Fig. 4. Arrival time of ground-level particles from one shower event in thunderstorm weather.

Fig. 5(a) shows the particle number as a function of arrival time during Thunderstorm 20220202 and in fair weather. Compared to the results in fair weather, the percent variation of particle number is shown in Fig. 5(b). It can be seen that the number increases during thunderstorms, especially for the arrival time larger than 400 ns, with a maximum value of about 8% at 800 ns. As a result, the triggered shower rate increases in strong electric fields.

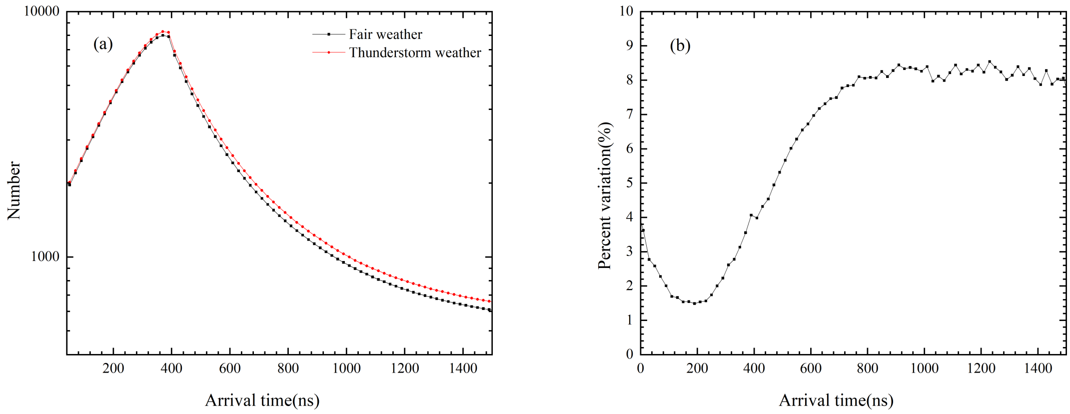

Fig. 5. Arrival time distribution (a) and percent variation (b) during Thunderstorm 20220202.

To better characterize the arrival time variation, the time distributions are normalized, as shown in Fig. 6(a). We can see that the arrival time distribution widens during Thunderstorm 20220202. For a better presentation of the results, the percent variations are shown in Fig. 6(b). When the arrival time is less than 550 ns, the percentage of particles decreases, with a maximum decrease of about -4.5%, otherwise the percentage of particles increases and the variation can be up to 2.1%.

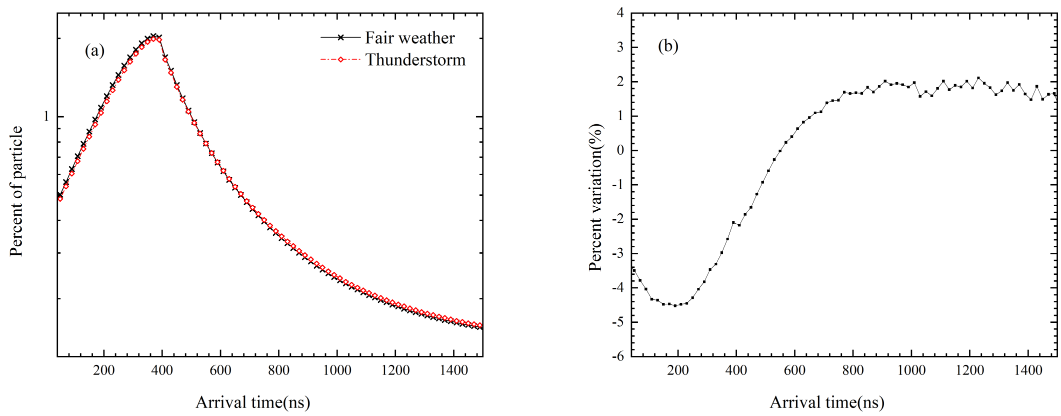

Fig. 6. Normalized arrival time distribution (a) and percent variation (b) during thunderstorms during Thunderstorm 20220202.

3.3 The AEF dependence of the arrival time variation

From above, we can see that the arrival time distribution widens during Thunderstorm 20220202. To study the relationship between the arrival time variation and the electric field strength, another thunderstorm that occurred on 7 June 2022 (called Thunderstorm 20220607 as shown in Fig. 7) is analyzed. This lasted for about two hours, with field strength exceeding 360 V/cm.

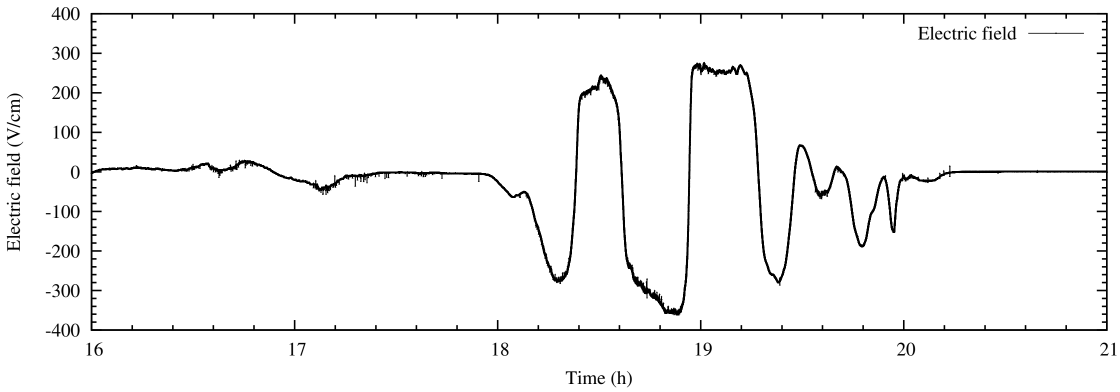

Fig. 7. Variation in the near-earth AEF during Thunderstorm 20220607.

We analyze the arrival time variations of secondary particles in different AEF strength ranges during Thunderstrom 20220607. Fig. 8(a) shows the normalized time distributions, and Fig. 8(b) shows the percentage variation of the particle arrival time. As shown in Fig. 8, near the trigger time region (less than 510 ns), the percentages of particles all decrease, and the decreasing amplitude increases with the AEF strength. However, the percentage of particles increases far from the trigger time, and the augmented magnitude is directly proportional to the intensity of the AEF. As the strength of the AEF intensities, the distribution of arrival time proportionally widens.

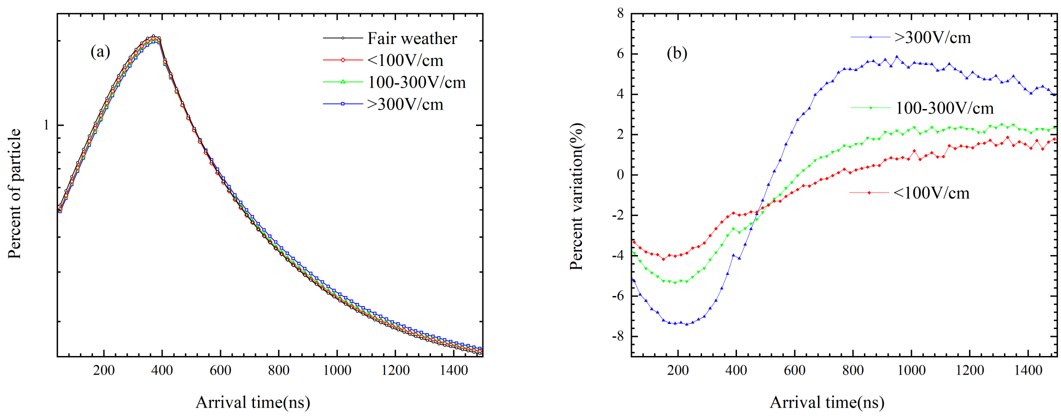

Fig. 8. Arrival time distribution (a) and percent variation (b) in different AEF strength ranges during Thunderstorm 20220607.

3.4 The zenith angle dependence of the arrival time variation

The AEFs have different effects on cosmic rays with different directions [13]. In this work, we study the variation of arrival time from different zenith angle ranges during thunderstorms. Firstly, the arrival time distributions in fair weather are analyzed, as shown in Fig. 9(a). It can be seen that the normalized arrival time distribution widens significantly with increasing zenith angle.

Compared with the results in fair weather, the percentage variations of the arrival time distributions in different zenith angle ranges during Thunderstorm 20220607 are shown in Fig. 9(b). The arrival time variations are found to be strongly dependent on the primary zenith angle. During the thunderstorm, near the trigger time region, the particle percentages decrease in all zenith angle ranges, and the decrease in amplitude increases with the zenith angle. Far from the trigger time, the opposite situation occurs, the particle percentages increase, and the amplitude increases with the zenith angle. As a result, the variation amplitude of the arrival time distribution becomes

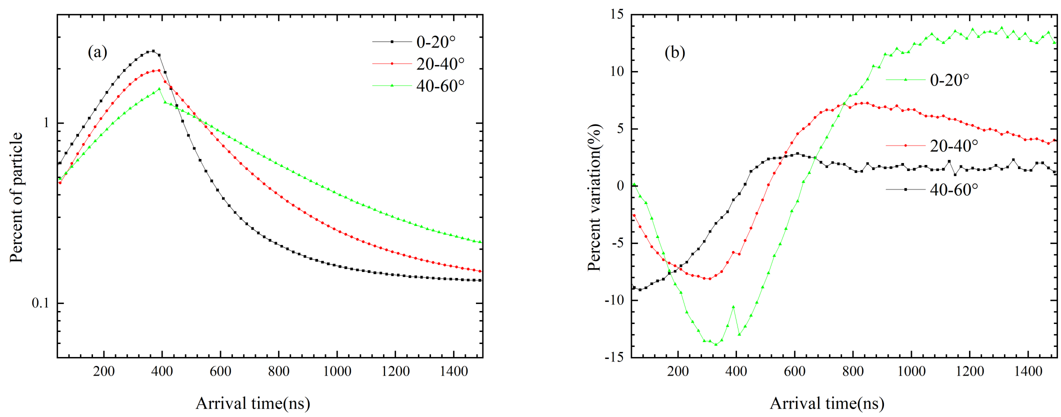

Fig. 9. Arrival time distribution (a) and percent variation (b) in different zenith angle ranges during Thunderstorm 20220607.

4. Summary

In this work, we have studied the arrival time distribution of the secondary particles in EAS detected by LHAASO-KM2A. Thunderstorm 20220202 and Thunderstorm 20220607 are chosen as typical examples. During thunderstorms, we can see that the arrival time distribution becomes wider, and the variation amplitude is dependent on the AEF strength and zenith angle. The arrival time distribution widens with the increase of the AEF strength, and the variation amplitude increases with the zenith angle.

Thunderstorm electric fields can widen the arrival time distribution. With the increase of AEF strength and zenith angle, the percentage of particles from the EAS decreases within a time window of 400 ns. As a result, the triggered shower rate and the shower reconstruction could be changed.

Acknowledgments

This work is supported by the National Natural Science Foundation of China (NSFC) under the Grant No. U2031101, and the National Key R&D Program of China under the grant No.2018YFA0404201. The authors would like to express their sincere thanks to the members of the LHAASO collaboration.

References

[1] X. S. Qie et al., Sci. China Earth Sci. **64**, 10 (2021).

[2] T. C. Marshall et al., Geophys. Res. Lett. **32**, L03813 (2005).

[3] Y. Y. Zhang et al., Journal of Sichuan Normal University **46**(4), 540-546 (2023).

[4] R. L. Huang et al., Journal of Sichuan Normal University **45**(6), 784-789 (2022).

[5] A. Chilingarian et al., Phys. Rev. D **103**, 043021 (2021).

[6] V. V. Alexeenko, N. S. Khaerdinov, A. S. Lidvansky et al., Phys. Lett. A **301**, 299-306 (2002).

[7] X. X. Zhou et al., Astropart. Phys. **84**, 107 (2016).

[8] K. Kudela, J. Chum, M. Kollárik, R. Langer, I. Strhárský, and J. Baše, J. Geophys. Res. **122**, 10700 (2017).

[9] J. Chum et al., Earth Planets Space **72**, D17 (2020).

[10] H. Y. Jia, L. Feng, D. Ruffolo et al., Chin. Phys. C, **46**, 030007 (2022).

[11] A. Chilingarian, G. Hovsepya, E. Svechnikova, and M. Zazyan, Astropart. Phys. **132**, 102615 (2021).

[12] R. R. Yan, D. H. Huang, B. Zhao, K. G. Axi, and X. X. Zhou, Chin. Astron. Astr. **44**, 146 (2020).

[13] K. G. Axi, X. X. Zhou, Z. C. Huang et al., Astrophys. Space Sci. **367**, 30 (2022).

[14] X. H. Ma, Y. J. Bi, Z. Cao et al., Chin. Phys. C **46**, 030001 (2022).

[15] F. Aharonian et al. (LHAASO Collaboration), Chin. Phys. C **47**, 015001(2023).

[16] L. Chen, K. G. Axi, X. X. Zhou et al., In: Proceedings of 37th ICRC, Berlin, Germany, July 12-23, 285 (2021).

[17] Peter K.F. Grieder., Springer, Berlin, Heidelberg, **1**, 7 (2009).

[18] G. Rastegarzadeh et al., Adv. Space Res. **65**, 2456–2466 (2020).

Full Authors List: LHAASO Collaboration

Zhen Cao[1,2,3], F. Aharonian[4,5], Q. An[6,7], Axikegu[8], Y.X. Bai[1,3], Y.W. Bao[9], D. Bastieri[10], X.J. Bi[1,2,3], Y.J. Bi[1,3], J.T. Cai[10], Q. Cao[11], W.Y. Cao[7], Zhe Cao[6,7], J. Chang[12], J.F. Chang[1,3,6], A.M. Chen[13], E.S. Chen[1,2,3], Liang Chen[14], Lin Chen[8], Long Chen[8], M.J. Chen[1,3], M.L. Chen[1,3,6], Q.H. Chen[8], S.H. Chen[1,2,3], S.Z. Chen[1,3], T.L. Chen[15], Y. Chen[9], N. Cheng[1,3], Y.D. Cheng[1,3], M.Y. Cui[12], S.W. Cui[11], X.H. Cui[16], Y.D. Cui[17], B.Z. Dai[18], H.L. Dai[1,3,6], Z.G. Dai[7], Danzengluobu[15], D. della Volpe[19], X.Q. Dong[1,2,3], K.K. Duan[12], J.H. Fan[10], Y.Z. Fan[12], J. Fang[18], K. Fang[1,3], C.F. Feng[20], L. Feng[12], S.H. Feng[1,3], X.T. Feng[20], Y.L. Feng[15], S. Gabici[21], B. Gao[1,3], C.D. Gao[20], L.Q. Gao[1,2,3], Q. Gao[15], W. Gao[1,3], W.K. Gao[1,2,3], M.M. Ge[18], L.S. Geng[1,3], G. Giacinti[13], G.H. Gong[22], Q.B. Gou[1,3], M.H. Gu[1,3,6], F.L. Guo[14], X.L. Guo[8], Y.Q. Guo[1,3], Y.Y. Guo[12], Y.A. Han[23], H.H. He[1,2,3], H.N. He[12], J.Y. He[12], X.B. He[17], Y. He[8], M. Heller[19], Y.K. Hor[17], B.W. Hou[1,2,3], C. Hou[1,3], X. Hou[24], H.B. Hu[1,2,3], Q. Hu[7,12], S.C. Hu[1,2,3], D.H. Huang[8], T.Q. Huang[1,3], W.J. Huang[17], X.T. Huang[20], X.Y. Huang[12], Y. Huang[1,2,3], Z.C. Huang[8], X.L. Ji[1,3,6], H.Y. Jia[8], K. Jia[20], K. Jiang[6,7], X.W. Jiang[1,3], Z.J. Jiang[18], M. Jin[8], M.M. Kang[25], T. Ke[1,3], D. Kuleshov[26], K. Kurinov[26], B.B. Li[11], Cheng Li[6,7], Cong Li[1,3], D. Li[1,2,3], F. Li[1,3,6], H.B. Li[1,3], H.C. Li[1,3], H.Y. Li[7,12], J. Li[7,12], Jian Li[7], Jie Li[1,3,6], K. Li[1,3], W.L. Li[20], W.L. Li[13], X.R. Li[1,3], Xin Li[6,7], Y.Z. Li[1,2,3], Zhe Li[1,3], Zhuo Li[27], E.W. Liang[28], Y.F. Liang[28], S.J. Lin[17], B. Liu[7], C. Liu[1,3], D. Liu[20], H. Liu[8], H.D. Liu[23], J. Liu[1,3], J.L. Liu[1,3], J.Y. Liu[1,3], M.Y. Liu[15], R.Y. Liu[9], S.M. Liu[8], W. Liu[1,3], Y. Liu[10], Y.N. Liu[22], R. Lu[18], Q. Luo[17], H.K. Lv[1,3], B.Q. Ma[27], L.L. Ma[1,3], X.H. Ma[1,3], J.R. Mao[24], Z. Min[1,3], W. Mitthumsiri[29], H.J. Mu[23], Y.C. Nan[1,3], A. Neronov[21], Z.W. Ou[17], B.Y. Pang[8], P. Pattarakijwanich[29], Z.Y. Pei[10], M.Y. Qi[1,3], Y.Q. Qi[11], B.Q. Qiao[1,3], J.J. Qin[7], D. Ruffolo[29], A. Sáiz[29], D. Semikoz[21], C.Y. Shao[17], L. Shao[11], O. Shchegolev[26,30], X.D. Sheng[1,3], F.W. Shu[31], H.C. Song[27], Yu.V. Stenkin[26,30], V. Stepanov[26], Y. Su[12], Q.N. Sun[8], X.N. Sun[28], Z.B. Sun[32], P.H.T. Tam[17], Q.W. Tang[31], Z.B. Tang[6,7], W.W. Tian[2,16], C. Wang[32], C.B. Wang[8], G.W. Wang[7], H.G. Wang[10], H.H. Wang[17], J.C. Wang[24], K. Wang[9], L.P. Wang[20], L.Y. Wang[1,3], P.H. Wang[8], R. Wang[20], W. Wang[17], X.G. Wang[28], X.Y. Wang[9], Y. Wang[8], Y.D. Wang[1,3], Y.J. Wang[1,3], Z.H. Wang[25], Z.X. Wang[18], Zhen Wang[13], Zheng Wang[1,3,6], D.M. Wei[12], J.J. Wei[12], Y.J. Wei[1,2,3], T. Wen[18], C.Y. Wu[1,3], H.R. Wu[1,3], S. Wu[1,3], X.F. Wu[12], Y.S. Wu[7], S.Q. Xi[1,3], J. Xia[7,12], J.J. Xia[8], G.M. Xiang[2,14], D.X. Xiao[11], G. Xiao[1,3], G.G. Xin[1,3], Y.L. Xin[8], Y. Xing[14], Z. Xiong[1,2,3], D.L. Xu[13], R.F. Xu[1,2,3], R.X. Xu[27], W.L. Xu[25], L. Xue[20], D.H. Yan[18], J.Z. Yan[12], T. Yan[1,3], C.W. Yang[25], F. Yang[11], F.F. Yang[1,3,6], H.W. Yang[17], J.Y. Yang[17], L.L. Yang[17], M.J. Yang[1,3], R.Z. Yang[7], S.B. Yang[18], Y.H. Yao[25], Z.G. Yao[1,3], Y.M. Ye[22], L.Q. Yin[1,3], N. Yin[20], X.H. You[1,3], Z.Y. You[1,3], Y.H. Yu[7], Q. Yuan[12], H. Yue[1,2,3], H.D. Zeng[12], T.X. Zeng[1,3,6], W. Zeng[18], M. Zha[1,3], B.B. Zhang[9], F. Zhang[8], H.M. Zhang[9], H.Y. Zhang[1,3], J.L. Zhang[16], L.X. Zhang[10], Li Zhang[18], P.F. Zhang[18], P.P. Zhang[7,12], R. Zhang[7,12], S.B. Zhang[2,16], S.R. Zhang[11], S.S. Zhang[1,3], X. Zhang[9], X.P. Zhang[1,3], Y.F. Zhang[8], Yi Zhang[1,12], Yong Zhang[1,3], B. Zhao[8], J. Zhao[1,3], L. Zhao[6,7], L.Z. Zhao[11], S.P. Zhao[12,20], F. Zheng[32], B. Zhou[1,3], H. Zhou[13], J.N. Zhou[14], M. Zhou[31], P. Zhou[9], R. Zhou[25], X.X. Zhou[8], C.G. Zhu[20], F.R. Zhu[8], H. Zhu[16], K.J. Zhu[1,2,3,6], X. Zuo[1,3], (The LHAASO Collaboration)

[1] Key Laboratory of Particle Astrophyics & Experimental Physics Division & Computing Center, Institute of High Energy Physics, Chinese Academy of Sciences, 100049 Beijing, China

[2] University of Chinese Academy of Sciences, 100049 Beijing, China

[3] TIANFU Cosmic Ray Research Center, Chengdu, Sichuan, China

[4] Dublin Institute for Advanced Studies, 31 Fitzwilliam Place, 2 Dublin, Ireland

[5] Max-Planck-Institut for Nuclear Physics, P.O. Box 103980, 69029 Heidelberg, Germany

[6] State Key Laboratory of Particle Detection and Electronics, China

[7] University of Science and Technology of China, 230026 Hefei, Anhui, China

[8] School of Physical Science and Technology & School of Information Science and Technology, Southwest Jiaotong University, 610031 Chengdu, Sichuan, China

[9] School of Astronomy and Space Science, Nanjing University, 210023 Nanjing, Jiangsu, China

[10] Center for Astrophysics, Guangzhou University, 510006 Guangzhou, Guangdong, China

[11] Hebei Normal University, 050024 Shijiazhuang, Hebei, China

[12] Key Laboratory of Dark Matter and Space Astronomy & Key Laboratory of Radio Astronomy, Purple Mountain Observatory, Chinese Academy of Sciences, 210023 Nanjing, Jiangsu, China

[13] Tsung-Dao Lee Institute & School of Physics and Astronomy, Shanghai Jiao Tong University, 200240 Shanghai, China

[14] Key Laboratory for Research in Galaxies and Cosmology, Shanghai Astronomical Observatory, Chinese Academy of Sciences, 200030 Shanghai, China

[15] Key Laboratory of Cosmic Rays (Tibet University), Ministry of Education, 850000 Lhasa, Tibet, China
[16] National Astronomical Observatories, Chinese Academy of Sciences, 100101 Beijing, China
[17] School of Physics and Astronomy (Zhuhai) & School of Physics (Guangzhou) & Sino-French Institute of Nuclear Engineering and Technology (Zhuhai), Sun Yat-sen University, 519000 Zhuhai & 510275 Guangzhou, Guangdong, China
[18] School of Physics and Astronomy, Yunnan University, 650091 Kunming, Yunnan, China
[19] Département de Physique Nucléaire et Corpusculaire, Faculté de Sciences, Université de Genève, 24 Quai Ernest Ansermet, 1211 Geneva, Switzerland
[20] Institute of Frontier and Interdisciplinary Science, Shandong University, 266237 Qingdao, Shandong, China
[21] APC, Université Paris Cité, CNRS/IN2P3, CEA/IRFU, Observatoire de Paris, 119 75205 Paris, France
[22] Department of Engineering Physics, Tsinghua University, 100084 Beijing, China
[23] School of Physics and Microelectronics, Zhengzhou University, 450001 Zhengzhou, Henan, China
[24] Yunnan Observatories, Chinese Academy of Sciences, 650216 Kunming, Yunnan, China
[25] College of Physics, Sichuan University, 610065 Chengdu, Sichuan, China
[26] Institute for Nuclear Research of Russian Academy of Sciences, 117312 Moscow, Russia
[27] School of Physics, Peking University, 100871 Beijing, China
[28] School of Physical Science and Technology, Guangxi University, 530004 Nanning, Guangxi, China
[29] Department of Physics, Faculty of Science, Mahidol University, Bangkok 10400, Thailand
[30] Moscow Institute of Physics and Technology, 141700 Moscow, Russia
[31] Center for Relativistic Astrophysics and High Energy Physics, School of Physics and Materials Science & Institute of Space Science and Technology, Nanchang University, 330031 Nanchang, Jiangxi, China
[32] National Space Science Center, Chinese Academy of Sciences, 100190 Beijing, China